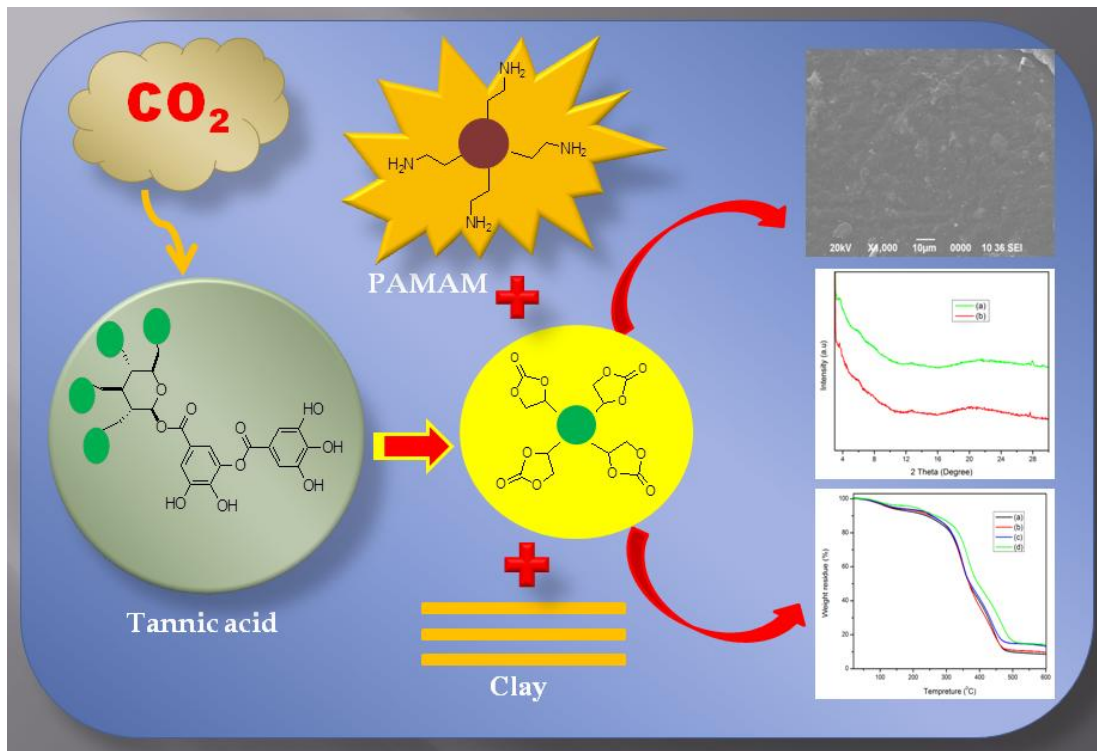# Chapter 6

Synthesis of tannic acid based polyurethane through non-isocyanate route and effect of organically modified clay on its physico-chemical behavior

This chapter describes the preparation of NIPU from bio-based tannic acid and its organically modified clay nanocomposites with improved mechanical properties

6.1 Introduction

Among the different polymeric materials, polyurethanes (PUs) are well-recognized owing to their exceptional versatility as they can be tailored for a large number of applications like adhesives, elastomers, surface coatings, tissue engineering, sensors and biomedical equipment [1–5]. However, conventionally, the PUs are synthesized by the addition polymerization of fossil source-based polyols and polyisocyanates [6,7]. So, an alternative greener route is most needed from these petroleum-based materials. For that reason, recently, in the production of polymers, the utilize of renewable resources for instance vegetable oils has gained importance as they are available worldwide, low price and environment-friendly in nature [8–10]. Recently, bio-based PUs are synthesized from various bio-based polyols (acquired from sunflower oil, castor oil, and soybean oil etc) by reacting it with polyisocyanates [11]. However, these isocyanates are synthesized from phosgenation of diamines which is unattractive because phosgene is a very toxic gas and longtime contact can create some bad health effects [12].

Therefore, PU development is focused on isocyanate free PUs and renewable resources which can compete with the fossil resource-based PUs. On this issues, the most favorable stand-in pathway is addition polymerization of polyamines with polycarbonates, leading to the non-isocyanate polyurethanes (NIPU) [13–17]. These cyclic carbonate are gained by the reaction of epoxides with CO_2 [18–21]. The main advantage of this chemical way is the substitution of phosgene by CO_2, an easily abundant and inexpensive resource [22]. Also, CO_2 is recognized as a one of the major greenhouse gases which origin the global warming and climate variation. Hence, the valorization of CO_2 for the preparation of essential materials is greatly helpful from the standpoint of utilization of renewable material and environmental.

This part of the thesis has been communicated

Doley, S. and Dolui, S. K. Synthesis of tannic acid based polyurethane through non-isocyanate route and effect of organically modified clay on its physicochemical behavior. *(Communicated)*

Recently NIPUs have been synthesized from various renewable raw material like vegetable oil, limonene and syringaresinol etc. [23–25]. Therefore in this study, we have developed bio-based NIPU by using tannic acid as a renewable raw material. Tannic acid is a readily available, water-soluble and high-molecular weight polyphenolic compound, and is generally extracted from plants as well as microorganisms. Its chemical structure consists of decagalloyl glucose core with phenolic hydroxyl groups [26,27] Besides, the properties of these tannic acid-based polymers is not suitable to achieve the high-performance applications such as engineering materials with regards to mechanical and thermal properties. From this perspective, the incorporation of nanomaterials plays a major role to enhance the properties of the pristine polymer. In recent years, polymer nanocomposites with nanoclays, such as montmorillonite (MC), have often been used to attain polymeric nanocomposites owing to its high aspect ratio, softness, superior mechanical properties, good solvent resistance, and low-priced and also because it is an earth-abundant inorganic nanomaterial [28,29]. Furthermore, the properties of polymer composites are highly dependent on the dispersion of the nano-fillers i.e. the low dispersion of nano-fillers results in poor properties of the nanocomposite. To resolve this difficulty, organic modifiers like silane are used to develop better compatibility between the nanoclay and the polymer matrix [29,30]. So in this work, to further enhance the properties of the prepared polymer, the nanoclays are functionalized with silane coupling agent 3-glycidoxypropyl trimethoxy silane (GPTMS) and then incorporated into the polymer matrix by varying amounts of modified clay (0.5, 1.0 and 1.5 wt% with respect to the resin).

6.2 Experimental

6.2.1 Materials

Tannic acid (Pure), 3-glycidoxypropyl trimethoxy silane (GPTMS) and MC were procured from Sigma-Aldrich and used as received. All the other chemicals used for the experiments are the same as explained in section 5.2.1 of Chapter 5.

6.2.2 Preparation of epoxidized tannic acid (ETAN)

The tannic acid based epoxy was prepared according to the method reported by Esmaeili et al [31]. Typically, tannic acid (6 g), epichlorohydrin (30 g), tetra-n-

butylammonium bromide (TBABr) (0.60 g) and distilled water (20.0 g) were put in a three-neck round bottom (RB) flask fitted with a thermometer and a condenser with constant stirring at 80 °C. After 1 h, to this reaction mixture, aqueous sodium hydroxide solution (20%) was added dropwise. The reaction was further continued for 3.5-4 h at 80 °C under constant stirring. After the desired time, the resulting mixture converted into a viscous mass and transferred into a separating funnel. The organic layers were separated and washed with 10% NaCl aq. solution and water 3-4 times. Finally, the resulting viscous mass was kept at 80 °C to evaporate excess epichlorohydrin and water. The epoxy equivalent weight (EEW) of the prepared ETAN was 535 ± 7 g mol^{-1}. The epoxy equivalent was calculated by titration methods.

6.2.3 Preparation of carbonated tannic acid (CTAN)

The cyclic carbonated tannic acid was prepared by reacting ETAN with CO_2 in a reactor at 75 °C and 50 bar pressure by using dimethylformamide (DMF) as the solvent and TBABr as the catalyst (10 wt% with respect to ETAN) for 16 h. The viscous cyclic carbonate product was precipitated out by adding water. The organic phase was collected and kept at 80 °C to get the final brownish viscous product.

6.2.4 Synthesis of cyclic carbonate functionalization of clay (CCLAY)

To synthesize cyclic carbonate clay (CCLAY), first, the cyclic carbonate derivative of GPTMS was prepared by reaction of GPTMS with CO_2 by using 10% (w/w) TBABr as the catalyst in a high-pressure reactor for 12 h under same reaction conditions as mentioned in the above procedure. Afterwards, the pressure was discharged and the carbonated product was collected. In the second step, 1 g of unmodified clay was dispersed in 100 mL of distilled water (solvent) at 50 °C. To the above mixture, 1 g of carbonated silane dissolved in 100 mL solvent was added and the dispersion was put under constant stirring for 2 h. The product clay (CCLAY) was filtered followed by washed with water and kept at 24 h at 60 °C to dry the product [32]. The schematic representation of the whole synthesis conversion process is shown in **Scheme 6.2**.

6.2.5 Preparation of tannic acid based NIPU (NPT)

NPT was synthesized by the reaction of CTAN with poly(amidoamine) (equivalent weight with respect to CTAN) at 70 °C for 3-4 h in DMF. The obtained product was kept on a Teflon sheet and maintained at 55 °C to take out the solvent. Then the resin was allowed to cure at 80 °C for 24 h and then post-curing occurred at 125-135 ^{0}C for 2 h to obtain completely cured films.

6.2.6 Preparation of NPT/CCLAY composites (NPTC)

The nanocomposites of NPT were prepared by incorporating CCLAY (0.5, 1.0 and 1.5 wt% compared to the resin). The CCLAY was first dispersed in DMF and after obtaining a stable dispersion, it was added to CTAN with continuous stirring at 70-75 °C for 3-4 h with the addition of poly(amidoamine). After completion of the reaction, the prepared composite was cured using the same process as mentioned above. NPTs with wt% 0.5, 1.0 and 1.5 of CCALY are designated as NPTC0.5, NPTC1.0 and NPTC1.0.

Table 6.1: Composition of the nanocomposites.

Sample name	CTAN (g)	Polyamidoamine (g)	CCLAY (mg)
NPT	2	2	0
NPTC0.5	2	2	20
NPTC1.0	2	2	40
NPTC1.5	2	2	60

*NPT stands for tannic acid based NIPU.

*NPTC stands for tannic acid based NIPU composites and the digit in NPTC represents the wt% of CCLAY added into the NPT.

6.2.7 Characterization

The instruments used for characterization including FT-IR, SEM, TGA, UTM, XRD, scratch hardness tester and titration methods of EEW determination are described in section 2.2.4 of chapter 2 and for XRD in section 3.2.6 of Chapter 3. The exploitation of clay was observed by using a transmission electron microscope (JEM-100 CX II). The chemical resistance of prepared films was evaluated by sinking small pieces of the cured in different types of solution.

6.3 Results and discussion

6.3.1 FT-IR studies

### 6.3.1.1 Preparation of ETAN and CTAN

ETAN was prepared by the reaction between tannic acid and epichlorohydrin in the presence of a base. This reaction is driven by the highly acidic nature of the phenolic protons of tannic acid. Here the active hydroxyl groups of tannic acid react with epichlorohydrin catalyzed by NaOH to give ETAN as shown in the **Scheme 6.1a**. The carbonation of ETAN was conducted in a high-pressure reactor at 75 °C and 50 bar for 16 h **(Scheme 6.1b)**.

The formation of cyclic carbonate (CTAN) groups was established by FT-IR analysis. In the FT-IR spectrum **(Fig. 6.1a)**, two characteristic peaks appear at around 895 cm^{-1} due to the epoxide groups of ETAN. The peaks appearing at around 1604 and 1240 cm^{-1} are the peaks of C=C bonds of aromatic ring and C-O of phenolic group respectively. The broad bands around 3442 and 1105 cm^{-1} are associated with hydroxyl groups of tannic acid and stretching C-O-C vibration of ether respectively. Regarding the reaction of ETAN with CO_2, the emergence of a new sharp signal at 1798 cm^{-1} **(Fig. 6.1b)** is attributed to the C=O vibration of the cyclic carbonate groups in CTAN.
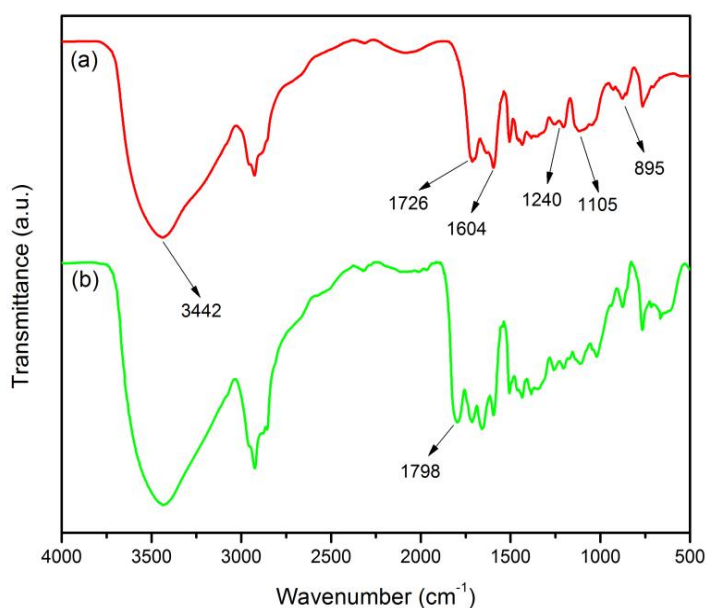
**Fig. 6.1:** FT-IR spectra of (a) ETAN and (b) CTAN.
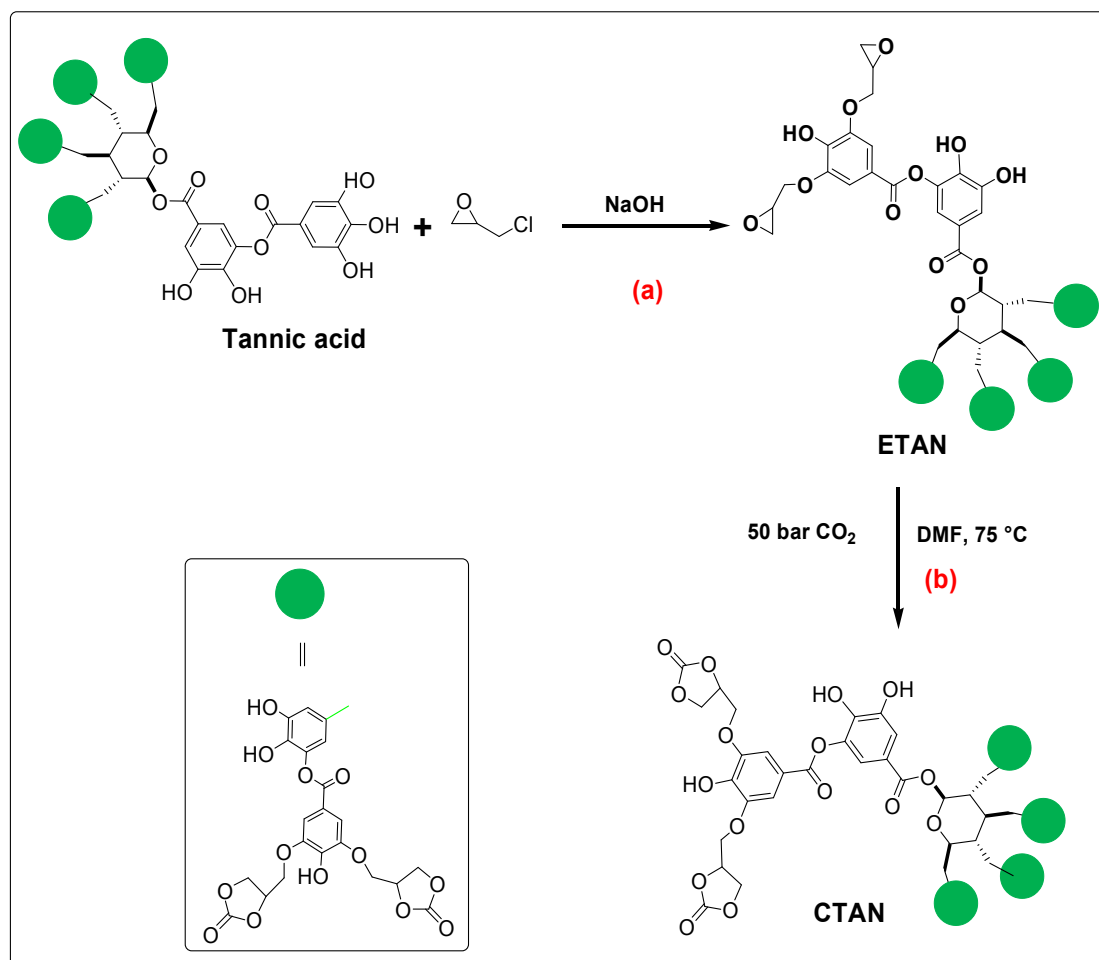
Scheme 6.1: (a) Formation of ETAN and (b) its reaction with CO_2 to form five-membered cyclic carbonate (CTAN).

6.3.1.2 Synthesis of CCLAY

The formation of carbonated silane (Csilane) and silane modified clay (CCLAY) were confirmed by FT-IR **(Fig. 6.2)** and shown in **Scheme 6.2**. In the FT-IR spectrum of Csilane (**Fig. 6.2a**), the band at 1796 cm^{-1} and the broad peak at 1098 cm^{-1} are ascribed to the carbonyl of the cyclic carbonate and Si-O stretching respectively [32]. Moreover, the bands at 1493, 793, and 693 cm^{-1} are attributed to Si-H, Si-O-C and -CH out-of-plane deformation. In the FT-IR spectrum of CCLAY (**Fig. 6.2b**), the characteristic peak at 1794 cm^{-1} along with other aforementioned peaks confirms the incorporation of Csilane into the clay. The two bands in the range 2843-2947 cm^{-1} in both the spectra are due to the -CH symmetric and asymmetric stretching of -CH$_2$ groups [28].
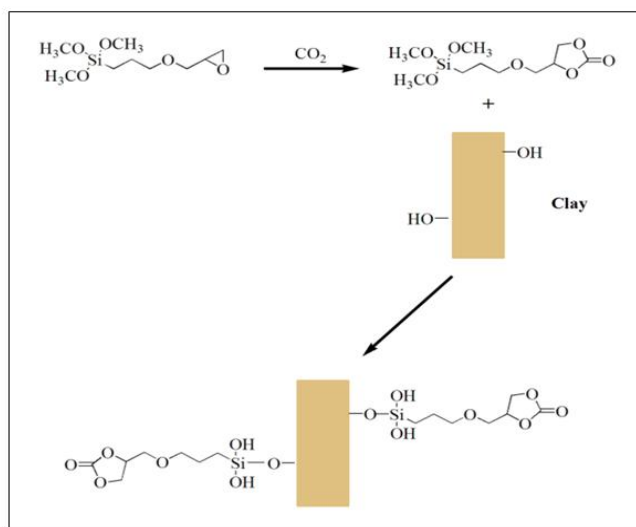
Scheme 6.2: Cyclic carbonate functionalized of clay (CCLAY).
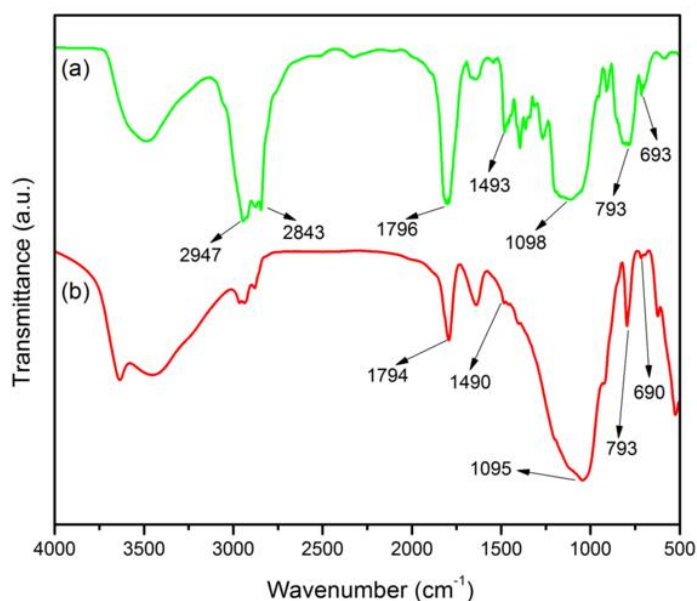
**Fig. 6.2:** FT-IR spectra of (a) Csilane and (b) CCLAY.

6.3.1.3 Preparation of NPT and NPTA/CCLAY composites (NPTC)

FT-IR spectra of NPT and NPTC0.5 are presented in **Fig. 6.3a** and **6.3b** respectively and shown in **Scheme 6.3**. In the FT-IR spectrum of NPT (**Fig. 6.3a**), the bands at 1706 cm^{-1} is attributed to the C=O stretching of urethane groups. The bands at 1653, 1546, 1252 and 1101 cm^{-1} correspond to C=C/amide group from polyamidoamine, N-H deformation of urethane group and C-N/C-O stretching vibration respectively. The absorption bands appearing at around 3426 cm^{-1} are related to O-H and N-H stretching.
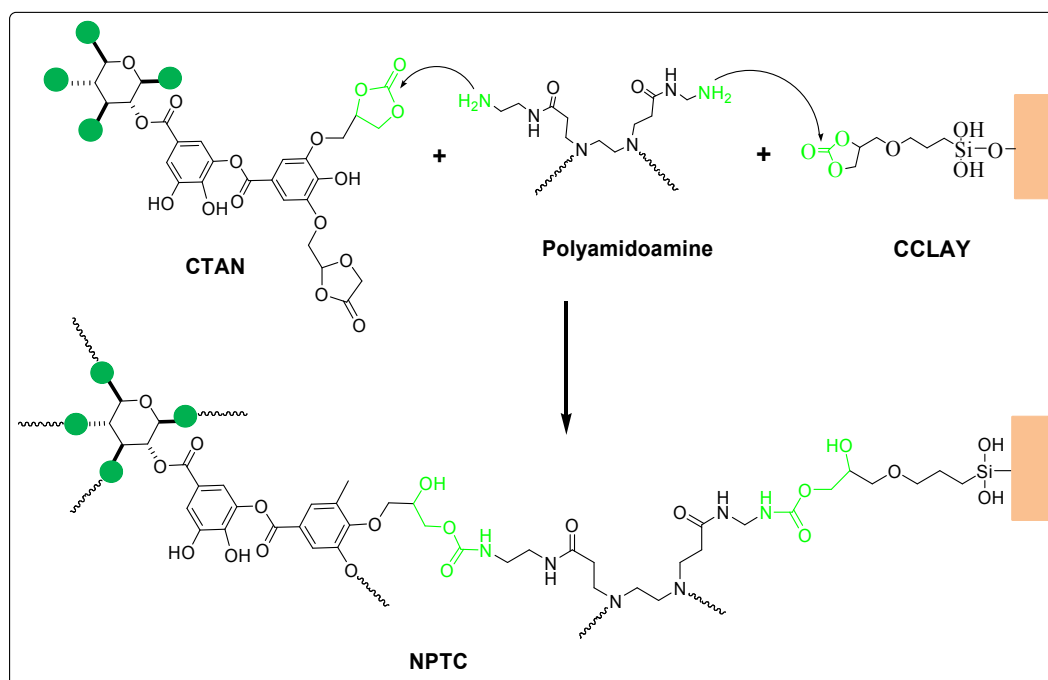
In the spectrum of NPTC0.5 **(Fig. 6.3b)**, the peak at 1796 cm^{-1} for cyclic carbonate in the CCLAY disappears. It confirms the formation of urethane bonds among the NPT, clay and polyamidoamine.
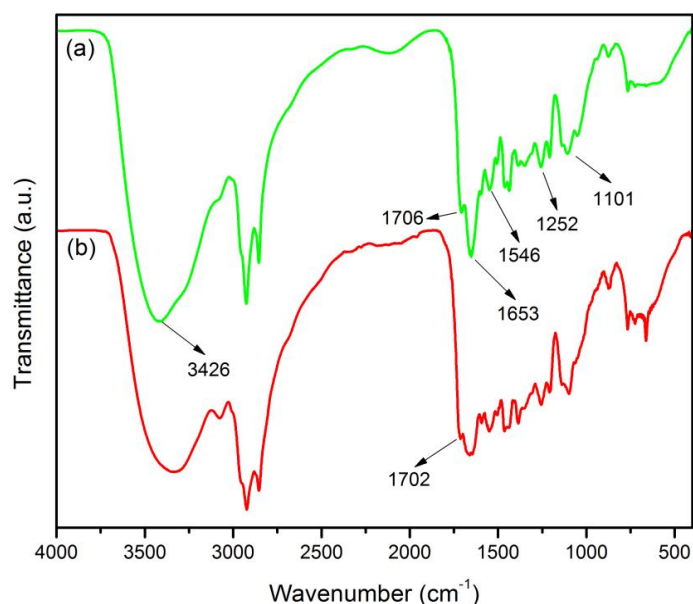
Fig. 6.3: FT-IR spectra of (a) NPT and (b) NPTC0.5.

Scheme 6.3: Reaction of CTAN and CCLAY with polyamidoamine to form NPT and NPTC.

6.3.2 XRD analysis

Fig. 6.4 presents the XRD patterns of unmodified clay and silane modified CCLAY. After incorporation of the CCLAY, the characteristic peak of pristine clays (001) **(Fig. 6.4a)** is shifted to lower 2θ value, suggesting that the grafting of carbonated silane into the layers of clays took place and results in the increased d-spacing of clay (18.5 Å). The increase of d-spacing reveals that the Csilane was grafted as well as intercalated in the layers of clay **(Fig. 6.4b)** [32].
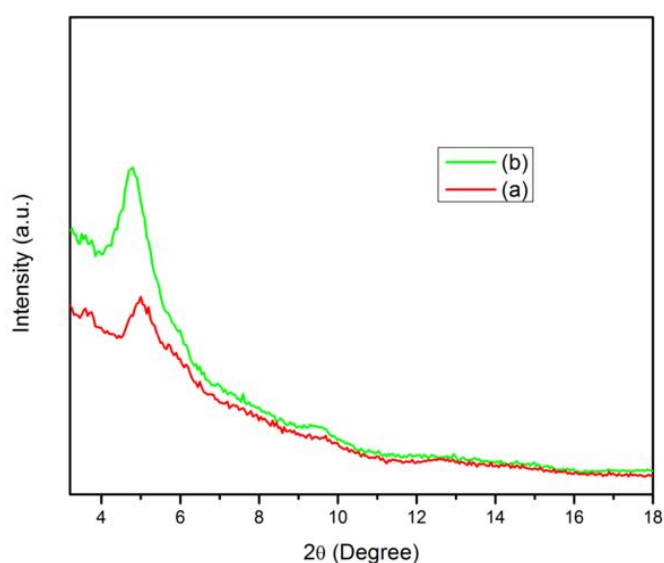

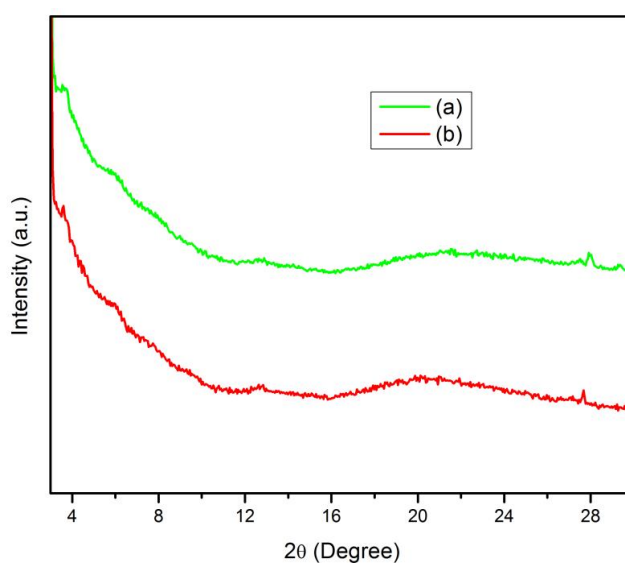**Fig. 6.4:** XRD curves of clays (a) unmodified clay and (b) CCLAY.


**Fig. 6.5:** XRD curves of clays (a) NPT and (b) NPTC1.0.

Fig. 6.5 represents the XRD patterns of the pristine NPT and its nanocomposites NPTC1.0. The NPT **(Fig. 6.5a)** exhibits a broad diffraction peak at around $2\theta = 21^\circ$. This diffraction pattern corresponds to the amorphous nature of NPT. The nanocomposite **(Fig. 6.5b)** also shows the same broad peak as that of the pristine polymer. No characteristic peak of the clays is observed in the nanocomposite which indicates that the clay platelets are fully exfoliated.

6.3.3 Morphological analysis

The surface morphologies of pure NPT and NPTC1.0 nanocomposite films were examined by SEM**. From **Fig. 6.6a**, it is seen that the prepared film shows a uniform surface morphology. In comparison to the pure NPT, the nanocomposite samples exhibit a rougher surface, due to the presence of rigid clays in the polymer matrix.
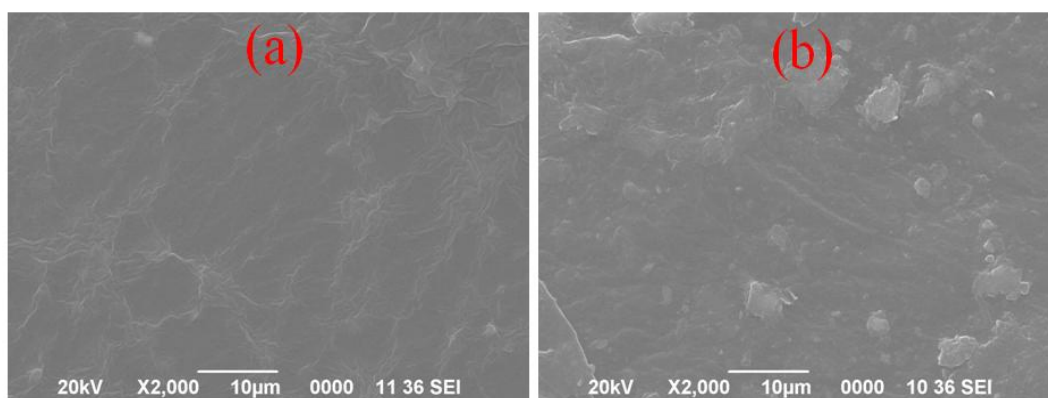
Fig. 6.6: SEM micrographs of (a) NPT and (b) NPTC1.0.
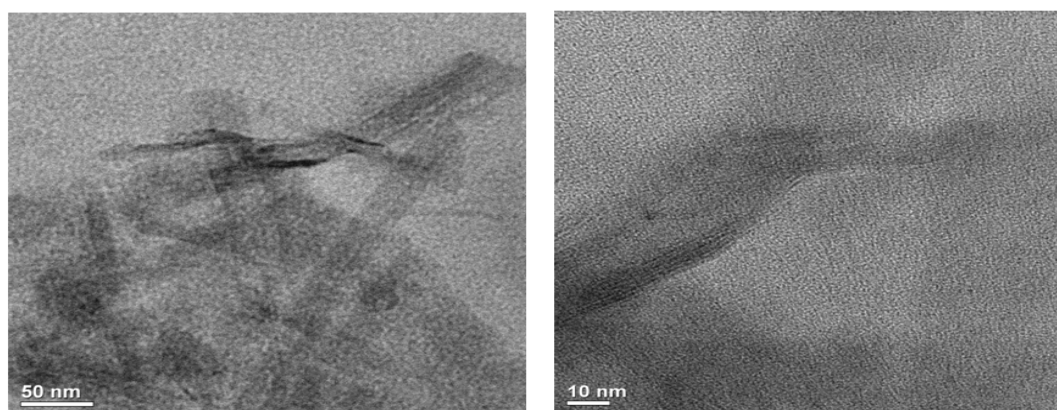
Fig. 6.7: TEM microphotograph of the NPTC1.0 nanocomposite at different magnifications.

The microstructure of NPTC1.0 nanocomposite was obtained by TEM analysis and the images are shown in **Fig. 6.7**. From the TEM micrograph, it is seen that the layers of clay are uniformly distributed and exploited within the polymer network which is in good agreement with the XRD study.

6.3.4 Mechanical properties

The mechanical performances of the prepared films are recorded in **Table 6.2**. From **Table 6.2**, it is seen that the addition of nanoclays significantly affects the mechanical properties of the nanocomposites. This is because of the increase in inter and intramolecular interactions between the macromolecular chains and the degree of hydrogen bonding. The reinforcement effect depends on the interactions between the polymer network and the dispersion of nanoclay. The tensile strength and scratch hardness is significantly enhanced with the incorporation of rigid clays due to the uniform dispersion of the carbonated clay (evidence from **Fig. 6.5b**). The highest tensile strength and scratch hardness are obtained for the sample with 1.5 wt % clay. The layered structure and chemical modification of clay make it easier to enhance the covalent cross-linking density and homogeneous distribution on the polymer matrix **(Scheme 6.3).**

Table 6.2: Mechanical properties of NPT and NPTC.

Sample Id	Tensile strength (MPa)	Elongation at break (%)	Scratch hardness (Kg)
NPT	5.6±0.2	35±2	4.5±0.2
NPTC0.5	7.8±0.1	41±2	5.3±0.1
NPTC1.0	8.2±0.1	37±1	5.6±0.2
NPTC1.5	8.8±0.2	30±3	6.0± 0.2

6.3.5 Thermal properties

Fig. 6.8 shows the TGA curves for NPT and its nanocomposites and the values are documented in **Table 6.3**. The results showed that the prepared NPT exhibits comparable thermal stability. In the case of NPT, the initial 10% weight loss (around 245

°C) can be related to the degradation of the urethane bonds and the ester groups of tannic acid.

With the incorporation of modified clays, the thermal stability of the nanocomposites is considerably improved. The interaction of nanoclay particles *via* chemical bonding with the polymer matrix by its cyclic carbonate group (as shown **Scheme 6.3**) may serve as a heat insulator resulting in the improvement of the thermal stability of the NPTC. Owing to the layered structure of the clay, it acts as a mass transport barrier, which slows down the degradation of the nanocomposites and release of the volatile products. Further, the hydroxyl group produced in the synthesis process of NPT can form hydrogen bonding with hydroxyl groups on the surfaces of clay, which additionally improves its stability.

Table 6.3: Thermal properties of NPT and its nanocomposites.

Sample Id	Temp @ 10% wt loss (°C)	Temp @ 25% wt loss (°C)	Temp @ 50% wt loss (°C)
NPT	245	326	369
NPTC0.5	252	328	368
NPTC1.0	258	329	373
NPTC1.5	267	349	396
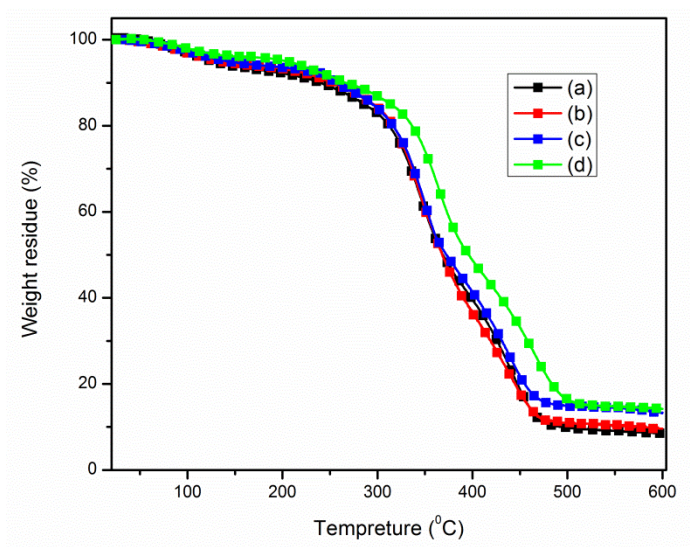
Fig. 6.8: TGA thermograms of (a) NPT, (b) NPTC0.5, (c) NPTC1.0 and (d) NPTC1.5.

6.3.6 Chemical properties

The chemical resistance test of NPT and its nanocomposites was carried out in HCl, NaCl, ethanol and NaOH by immersion method and the results are summarized in **Table 6.4**. The prepared NPT and NPTCs exhibit excellent resistance to acid, ethanol and salt solution. Here, the chemical resistance properties in the cured films can be credited to the highly crosslinked structure and strong hydrogen bonding interactions of the functional groups present in the polymer networks. But due to the presence of hydrolyzable ester linkages in tannic acid, the alkali resistance is simply fair. However, due to the formation of nanocomposites of rigid clay and aromatic nature of tannic acid, the solvent penetration is forbidden and the nanocomposites display suitable resistance to alkali.

Table 6.4: Chemical resistances of NPT and NPTC.

Sample Id	HCl (10%)	Ethanol (25%)	NaCl (10%)	NaOH (5%)
NPT	Excellent	Excellent	Excellent	Fair
NPTC0.5	Excellent	Excellent	Excellent	Good
NPTC1.0	Excellent	Excellent	Excellent	Good
NPTC1.5	Excellent	Excellent	Excellent	Good

*Excellent= No weight loss

6.4 Conclusion

In this study, bio-based polyurethane was synthesized via novel isocyanate-free routes by using CO_2 and tannic acid. Tannic acid-based cyclic carbonates were first obtained by the reactions of CO_2 with epoxidized tannic acid under pressure 50 bar at 75 °C. This cyclic carbonated tannic acid was then reacted with poly(amido amine) to obtain tannic acid-based NIPUs. The prepared resins were successfully characterized and finally, the nanocomposites of the NPT were prepared using organically modified clay. The prepared nanocomposites showed better performance than the pure polymer. The chemical interactions and strong hydrogen bonding of clay with the polymer matrix resulted in improved performance of the nanocomposites. The prepared composites exhibited better mechanical, thermal and chemical properties than pure NPT.

6.5 References

[1]   Kausar, A. Polyurethane nanocomposite coatings: state of the art and perspectives. *Polymer International*, 67(11):1470-1477, 2018.

[2]   Król, P. Synthesis methods, chemical structures and phase structures of linear polyurethanes. Properties and applications of linear polyurethanes in polyurethane elastomers, copolymers and ionomers. *Progress in Materials Science*, 52(6):915-1015, 2007.

[3]   Zdrahala, R. J. and Zdrahala, I. J. Biomedical applications of polyurethanes: A review of past promises, present realities, and a vibrant future. *Journal of Biomaterials Applications*, 14(1):67-90, 1999.

[4]   Chattopadhyay, D. K. and Raju, K. V. S. N. Structural engineering of polyurethane coatings for high performance applications. *Progress in Polymer Science*, 32(3):352-418, 2007.

[5]   Pelrine, R. E., Kornbluh, R. D., and Joseph, J. P. Electrostriction of polymer dielectrics with compliant electrodes as a means of actuation. *Sensors and Actuators A: Physical*, 64(1):77-85, 1998.

[6]   Kong, X., Liu, G., and Curtis, J. M. Novel polyurethane produced from canola oil based poly(ether ester) polyols: Synthesis, characterization and properties. *European Polymer Journal*, 48(12):2097-2106, 2012.

[7]   Garrison, T. F., Kessler, M. R., and Larock, R. C. Effects of unsaturation and different ring-opening methods on the properties of vegetable oil-based polyurethane coatings. *Polymer*, 55(4):1004-1011, 2014.

[8]   Doley, S. and Dolui, S. K. Solvent and catalyst-free synthesis of sunflower oil based polyurethane through non-isocyanate route and its coatings properties. *European Polymer Journal*, 102:161-168, 2018.

[9]   Gogoi, P., Boruah, M., Sharma, S., and Dolui, S. K. Blends of epoxidized alkyd resins based on jatropha oil and the epoxidized oil cured with aqueous citric acid solution: A Green technology approach. *ACS Sustainable Chemistry & Engineering*, 3(2):261-268, 2015.

[10]   Palaskar, D. V., Boyer, A., Cloutet, E., Le Meins, J. F., Gadenne, B., Alfos, C., Farcet, C., and Cramail, H. Original diols from sunflower and ricin oils: Synthesis, characterization, and use as polyurethane building blocks. *Journal of Polymer*

Science Part A: Polymer Chemistry, 50(9):1766-1782, 2012.

[11] Carme Coll Ferrer, M., Babb, D., and Ryan, A. J. Characterisation of polyurethane networks based on vegetable derived polyol. *Polymer*, 49(15):3279-3287, 2008.

[12] Maisonneuve, L., Wirotius, A. L., Alfos, C., Grau, E., and Cramail, H. Fatty acid-based (bis) 6-membered cyclic carbonates as efficient isocyanate free poly(hydroxyurethane) precursors. *Polymer Chemistry*, 5(21):6142-6147, 2014.

[13] Beniah, G., Uno, B. E., Lan, T., Jeon, J., Heath, W. H., Scheidt, K. A., and Torkelson, J. M. Tuning nanophase separation behavior in segmented polyhydroxyurethane via judicious choice of soft segment. *Polymer*, 110:218-227, 2017.

[14] Tryznowski, M., Świderska, A., Żołek-Tryznowska, Z., Gołofit, T., and Parzuchowski, P. G. Facile route to multigram synthesis of environmentally friendly non-isocyanate polyurethanes. *Polymer*, 80:228-236, 2015.

[15] Maisonneuve, L., Lamarzelle, O., Rix, E., Grau, E., and Cramail, H. Isocyanate-free routes to polyurethanes and poly(hydroxy urethane)s. *Chemical Reviews*, 115(22):12407-12439, 2015.

[16] Doley, S., Sarmah, A., Sarkar, C., and Dolui, S. K. *In situ* development of bio-based polyurethane- *blend* -epoxy hybrid materials and their nanocomposites with modified graphene oxide via non-isocyanate route. *Polymer International*, 67(8):1062-1069, 2018.

[17] Dolci, E., Michaud, G., Simon, F., Boutevin, B., Fouquay, S., and Caillol, S. Remendable thermosetting polymers for isocyanate-free adhesives: a preliminary study. *Polymer Chemistry*, 6(45):7851-7861, 2015.

[18] Dolci, E., Froidevaux, V., Michaud, G., Simon, F., Auvergne, R., Fouquay, S., and Caillol, S. Thermoresponsive crosslinked isocyanate-free polyurethanes by Diels-Alder polymerization. *Journal of Applied Polymer Science*, 134(5):2017.

[19] Esmaeili, N., Zohuriaan-Mehr, M. J., Salimi, A., Vafayan, M., and Meyer, W. Tannic acid derived non-isocyanate polyurethane networks: Synthesis, curing kinetics, antioxidizing activity and cell viability. *Thermochimica Acta*, 664:64-72, 2018.

[20] Nanclares, J., Petrović, Z. S., Javni, I., Ionescu, M., and Jaramillo, F. Segmented polyurethane elastomers by nonisocyanate route. *Journal of Applied Polymer*

Science, 132(36):42492, 2015.

[21] Mazurek-Budzyńska, M. M., Rokicki, G., Drzewicz, M., Guńka, P. A., and Zachara, J. Bis(cyclic carbonate) based on d-mannitol, d-sorbitol and di(trimethylolpropane) in the synthesis of non-isocyanate poly(carbonate-urethane)s. *European Polymer Journal*, 84:799-811, 2016.

[22] Xu, S., Li, C., Li, H., Li, M., Qu, C., and Yang, B. Carbon dioxide sensors based on a surface acoustic wave device with a graphene-nickel-l -alanine multilayer film. *Journal of Materials Chemistry C*, 3(16):3882-3890, 2015.

[23] Tamami, B., Sohn, S., and Wilkes, G. L. Incorporation of carbon dioxide into soybean oil and subsequent preparation and studies of nonisocyanate polyurethane networks. *Journal of Applied Polymer Science*, 92(2):883-891, 2004.

[24] Boyer, A., Cloutet, E., Tassaing, T., Gadenne, B., Alfos, C., and Cramail, H. Solubility in CO_2 and carbonation studies of epoxidized fatty acid diesters: towards novel precursors for polyurethane synthesis. *Green Chemistry*, 12(12):2205, 2010.

[25] Maisonneuve, L., More, A. S., Foltran, S., Alfos, C., Robert, F., Landais, Y., Tassaing, T., Grau, E., and Cramail, H. Novel green fatty acid-based bis-cyclic carbonates for the synthesis of isocyanate-free poly(hydroxyurethane amide)s. *RSC Advances*, 4(49):25795-25803, 2014.

[26] Lin, H., Pei, L., and Zhang, L. Enhanced thermal conductivity of PLA-based nanocomposites by incorporation of graphite nanoplatelets functionalized by tannic acid. *Journal of Applied Polymer Science*, 135(26):46397, 2018.

[27] Liu, W., Qiu, J., Zhu, L., Fei, M., Qiu, R., Sakai, E., Ito, K., Song, G., and Tang, G. Tannic acid-induced crosslinking of epoxidized soybean oil for toughening poly(lactic acid) via dynamic vulcanization. *Polymer*, 148:109-118, 2018.

[28] Liao, L., Li, X., Wang, Y., Fu, H., and Li, Y. Effects of surface structure and morphology of nanoclays on the properties of jatropha curcas oil-based waterborne polyurethane/clay nanocomposites. *Industrial & Engineering Chemistry Research*, 55(45):11689-11699, 2016.

[29] Yebassa, D., Balakrishnan, S., Feresenbet, E., Raghavan, D., Start, P. R., and Hudson, S. D. Chemically functionalized clay vinyl ester nanocomposites: Effect of processing parameters. *Journal of Polymer Science Part A: Polymer Chemistry*,

42(6):1310-1321, 2004.

[30] Alateyah, A. I., Dhakal, H. N., and Zhang, Z. Y. Processing, properties, and applications of polymer nanocomposites based on layer silicates: A Review. *Advances in Polymer Technology*, 32(4):2013.

[31] Esmaeili, N., Vafayan, M., Salimi, A., and Zohuriaan-Mehr, M. J. Kinetics of curing and thermo-degradation, antioxidizing activity, and cell viability of a tannic acid based epoxy resin: From natural waste to value-added biomaterial. *Thermochimica Acta*, 655:21-33, 2017.

[32] Huskić, M., Žigon, M., and Ivanković, M. Comparison of the properties of clay polymer nanocomposites prepared by montmorillonite modified by silane and by quaternary ammonium salts. *Applied Clay Science*, 85:109-115, 2013.